

## Determination of Power System Risk by Means of Bootstrap Technique

<sup>1</sup>S.R. Kasim, <sup>1</sup>M.M. Othman, <sup>1</sup>N.F.A. Ghani, <sup>1</sup>I. Musirin, <sup>2</sup>A. Mohammed and <sup>2</sup>A. Hussain

<sup>1</sup>Faculty of Electrical Engineering, Universiti Teknologi MARA 40450 Shah Alam, Selangor, Malaysia.

<sup>2</sup>Department of Electrical, Electronic and Systems Engineering, Faculty of Engineering & Built Environment, Universiti Kebangsaan Malaysia 43600 Bangi, Selangor, Malaysia.

---

**Abstract:** This paper presents the risk assessment of power system that takes into account the system failure indices and uncertainty of unavailable load variations estimated by using the fuzzy set and bootstrap technique. The risk of the system is measured by using the expected energy not supplied (EENS) index as well as the probability of load curtailment (PLC). The bootstrap technique is a tool which provides simplest way to perform risk assessment of a power system compared to the fuzzy set. Furthermore, it also requires very little assumptions to carry-out the risk analysis and it is imperative especially for a small size of available information. The application of bootstrap technique is important to assess the risk indices at every level of system uncertainty. The 24-bus IEEE Reliability Test System (RTS) is used as a case study in the analysis of system risk severity based EENS and PLC. Comparative studies have been made on the risk assessment of the power system determined by using the bootstrap technique, fuzzy set and; the combined fuzzy set and bootstrap technique.

**Key words:** Fuzzy set; bootstrap technique; risk assessment; expected energy not supplied (EENS); probability of load curtailment (PLC).

---

### INTRODUCTION

In recent years, immense power system outage events have happened across the world. This is not exceptional to the Malaysia power system whereby on January 13, 2005 the system blackout occurred due to cascading overloads (KL, 2005). Similar incident happened in New York plunging up to nine million people into darkness due to lightning struck at the tower line in Northern Westchester [2]. Hence, there have been efforts devoted in searching new methods and procedures that effectively evaluate the risk of a power system considering various consequences (Li, 2005; Billinton and Li, 1994; IEEE, 2005; Schilling, 1990; Allan *et al.*, 1999; Billinton *et al.*, 2001; Framework, 1998; Marceau and Endrenyi, 1997; Singh and Fouad *et al.*, 1997; Calley *et al.*, 1997).

The risk assessment of a power system is usually performed by using a probabilistic approach. Randomness and fuzziness are the two types of uncertainty that exist in power system. Fuzziness can be described as the ambiguity of an event, whereas randomness represents as numerous occurrences of event Kosko, (1990). Randomness in power system components can be modeled by using the probabilistic approach.

In a conventional approach of risk assessment, the failure indices such as repair time and failure frequency of a component are often modeled at mean value. However, assessing the risk of a system should consider the probability distribution of failure indices rather than just by considering its mean value Li, (2005). On the other hand, there are several drawbacks in using the probability distribution of failure indices for the risk assessment in power system. Whereby, it is difficult to design the probability distribution for failure indices due to limited statistical record of information. This yields to the fuzziness representation of failure indices that cannot be presented in terms of probability distribution. It is recognized that the failure rate of an outdoor component is uncertain or fuzzy due to weather effect (Schilling, 1990; Billinton and Li, 1992). Normally, weather conditions can be considered as fuzzy and it can be categorized as heavy, medium, or light. For this reason, fuzzy model can be used as a tool in providing uncertain failure indices for the risk assessment of a power system.

---

**Corresponding Author:** M.M. Othman, Faculty of Electrical Engineering, Universiti Teknologi MARA 40450 Shah Alam, Selangor, Malaysia.

The bootstrap technique can be used to represent the uncertain conditions of failure indices as well as the risk assessment of a power system. It is a resampling based method developed by Efron that has been used extensively in statistical problems Bradley and Tibshirani, (1994). The bootstrap technique is robust in estimating the uncertainty based on a small sample size of system parameters Othman *et al.*, (2008). The uncertainty of system parameters are significant to be used in the risk assessment of power system. This method also has been used to solve many other problems that would be too complicated for traditional approach.

The applications of bootstrap technique in the risk assessment on various case studies have been reported in previous papers. S. Alborzi *et al.* (2008) explained the motivations for using bootstrap technique in typical risk analysis. F. Verdonck *et al.* (2000) presents the bootstrap technique that used to determine the uncertainty for environmental risk assessment.

The risk assessment of a power system due to the occurrence of catastrophic system failures determined by using bootstrap technique was presented in Mili *et al.*, (2004).

This paper presents the bootstrap technique that used to access the risk of a system. The risk assessment of a power system is performed by considering the uncertainty of system states and uncertain load conditions determined by using the bootstrap technique. On the other hand, the fuzzy set has also been used to perform the risk analysis of a power system. The risk assessment of a power system is performed by considering the uncertainty of system states and uncertain load conditions determined by the fuzzy set. The risk of a power system is evaluated based on the expected energy not supplied (EENS) and probability of load curtailment (PLC). A 24-bus IEEE Reliability Test System (RTS) is used to verify the effectiveness of the proposed method in power system risk assessment. Comparative studies have been made on the risk assessment of the power system determined by using the bootstrap technique, fuzzy set and; the combined fuzzy set and bootstrap technique. The bootstrap technique has the advantage of elucidating the results of system risk at every uncertainty of bootstrap confidence interval.

***Fuzzy Model for Outage Parameters:***

The fuzzy model plays an important role to overcome insufficient or uncertain probability distribution of failure indices. The model for failure indices is characterized by its fuzzy model of failure frequency and repair time. The following subsections provide detail explanations on the fuzzy models of repair time, failure frequency and outage or unavailability for a component.

***Fuzzy Model for Repair Time:***

The sample mean is a popular estimation for modeling the repair time. Equation (1) represents the average repair time for outage events of a component.

$$\bar{r} = \frac{1}{NO} \sum_{k=1}^{NO} r_k \tag{1}$$

where,

$\bar{r}$  : point estimate of repair time.

$r_k$  :  $k^{\text{th}}$  repair time.

$NO$  : total number of repair times for outage component.

The confidence range of estimated parameter is then determined by using the student-*t* distribution. The student-*t* distribution is used suitable for estimating the confidence range of a small sample population size William, (2006).

Assume that,  $\mu$ , is the expected repair time and,  $s$ , is the standard deviation for a sample of repair time. According to statistical theory, for a given significant level  $\alpha$ , it can be affirmed that the random variable

$\left[ \frac{(\bar{r}-\mu)}{s/\sqrt{n}} \right]$  is located between  $-t_{\alpha/2}(n-1)$  and  $t_{\alpha/2}(n-1)$  with the probability confidence interval of

$1 - \alpha$  Therefore,

$$-t_{\alpha/2}(n-1) \leq \frac{\bar{r} - \mu}{s/\sqrt{n}} \leq t_{\alpha/2}(n-1) \tag{2}$$

Equation (2) can be expressed as,

$$r_4 = \bar{r} - t_{\alpha/2}(n-1) \frac{s}{\sqrt{n}} \leq \mu \leq \bar{r} + t_{\alpha/2}(n-1) \frac{s}{\sqrt{n}} = r_5 \tag{3}$$

Hence, it is equivalent to

$$r_4 = \bar{r} - t_{\alpha/2}(n-1) \frac{s}{\sqrt{n}} \tag{4}$$

and

$$r_5 = \bar{r} + t_{\alpha/2}(n-1) \frac{s}{\sqrt{n}} \tag{5}$$

Equations (4) and (5) indicate that the expected repair time is located between the lower and upper bounds of the sample, respectively. By having the confidence of repair time, triangle membership function of repair time,  $r$ , can be obtained as shown in Fig. 1. The point estimate  $r$  is corresponding to 1.0 of the membership function grade. The significant level  $\alpha$  is always in a small percentage such as 5% or 0.05. The half of  $\alpha$  is located near to the end of the two bounds in  $t$ -distribution. Conceptually, the significant level is relatively similar to the fuzzy degree that used to estimate the confidence range of fuzzy. Therefore, it can be assumed that the lower bound of  $r_4$  and upper bound of  $r_5$ , obtained from equations (4) and (5), respectively are

corresponding to the points having a membership grade of  $\alpha/2$ . Then, the three points of  $(r_4, \alpha/2)$ ,  $(\bar{r}, 1.0)$ , and  $(r_5, \alpha/2)$  are used in the linear algebraic equation of  $y = mx + c$  to obtain the two end points of  $(r_1, 0)$  and  $(r_3, 0)$  in the fuzzy membership function. When the value of  $\alpha/2$  is very small for instance 0.025,

the values of  $r_1$  is relatively similar to  $r_4$  at the lower bound of fuzzy membership function. This situation is similar to  $r_3$  and  $r_5$ . Wherein, a small value of  $\alpha/2 = 0.025$  yields  $r_3$  that is relatively similar to  $r_5$  at the upper bound of fuzzy membership function. Therefore,  $r_1$  and  $r_4$  can be used as the two end points at lower bound of fuzzy membership function. On the other side,  $r_5$  and  $r_3$  can be used as the two end points at upper bound of fuzzy membership function. It can be seen in Fig. 1 that the fuzzy membership function comprises of lower bound that is symmetrical to the upper bound.

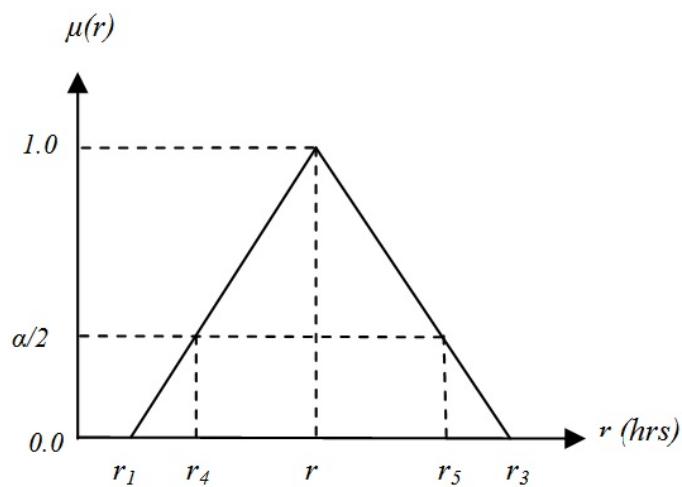


Fig. 1: Membership function of repair time.

**Fuzzy Model for Failure Frequency:**

The failure frequency of a component is usually estimated as an average value. Equation (6) shows the point estimate of failure frequency for a component.

$$\bar{f} = \frac{N_f}{T} \tag{6}$$

where,

$N_f$  : number of repairable failures of a component in the time period,  $T$ . Whereby,  $T = 1$  year or it is equivalent to 8760 hours IEEE, (1979).

According to statistical theory, there exist a relationship between the  $\chi^2$  distribution and Poisson distribution Li, (2005).

$$\chi^2(2F) = 2\lambda T \tag{7}$$

where,

$\lambda$  : failure rate.

$T$  : total time period.

$F$  : number of failures during .

Equation (7) shows that the quantity with two times of expected failures in duration  $T$  is equivalent to the  $\chi^2$  distribution with  $2F$  degree of freedom Li, (2005).

Therefore, for a given significance level,  $\alpha$ , it can be asserted that the failure rate,  $\lambda$  falls into the following confidence interval.

$$\frac{\chi^2_{(1-\alpha/2)}(2F)}{2T} \leq \lambda \leq \frac{\chi^2_{(\alpha/2)}(2F)}{2T} \tag{8}$$

Equation (8) gives the lower and higher bounds of failure frequency. The  $f$  and  $\lambda$  are numerically very similar and it is frequently replaced between each other in practical engineering calculations of power system risk assessment (Li, 2005; Billinton and Li, 1994). Therefore, equation (8) can be used to estimate the two bounds of failure frequency,  $f$ . Hence, equation (8) can be written as:

$$\frac{\chi^2_{(1-\alpha/2)}(2F)}{2T} \leq f \leq \frac{\chi^2_{(\alpha/2)}(2F)}{2T} \tag{9}$$

Equation (9) can be expressed as,

$$f_4 = \frac{\chi^2_{(1-\alpha/2)}(2F)}{2T} \leq f \leq \frac{\chi^2_{(\alpha/2)}(2F)}{2T} = f_5 \tag{10}$$

Equation (10) indicates that the failure frequency is located between the lower bound and upper bound of the sample. A triangle membership function of failure frequency can be easily drawn by using three points of  $(f_4, \alpha/2)$ ,  $(f, 1.0)$ , and  $(f_5, \alpha/2)$ . Two end points of  $(f_4, 0)$  and  $(f_5, 0)$  can be obtained by using linear algebraic equation of  $y=mx+c$ . Note that the membership function of failure frequency is not symmetric as shown in Fig. 2. Generally, the range of upper bound is much larger than the range of lower bound.

**Fuzzy Model for Unavailability:**

The unavailability,  $U$  of a component can be calculated by considering the failure frequency and repair time, and it is given in equation (11).

$$U = \frac{f \times r}{8760} \tag{11}$$

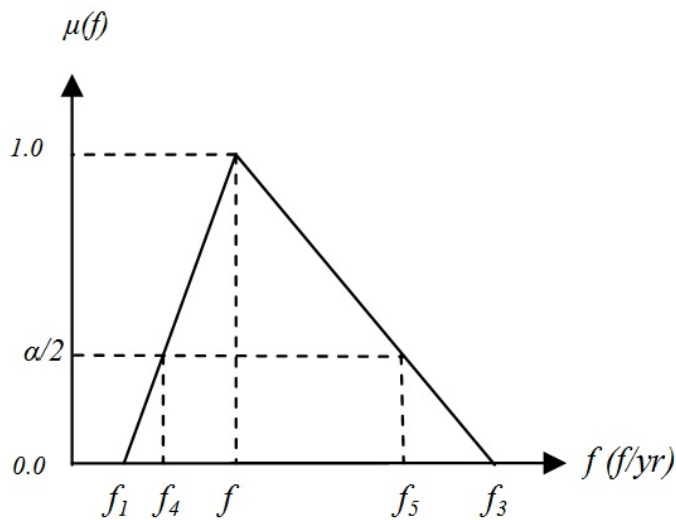


**Fig. 2:** Membership function of failure frequency.

The units for failure frequency,  $f$ , and repair time,  $r$  are failures/year and hours/failure, respectively. The fuzzy membership function of unavailability can be calculated by considering the fuzzy membership functions of failure frequency and repair time as shown in Fig. 1 and Fig. 2, respectively. There are several basic rules in the calculation involving two fuzzy membership functions as given in equations (12)-(16). The intervals  $V$  and  $W$ , and constant  $h$  are considered in the calculations.

$$V + W = [v_1, v_2] + [w_1, w_2] = [v_1 + w_1, v_2 + w_2] \tag{12}$$

$$V - W = [v_1, v_2] - [w_1, w_2] = [v_1 - w_1, v_2 - w_2] \tag{13}$$

$$V \times W = [v_1, v_2] \times [w_1, w_2] = [v_1 \times w_1, v_2 \times w_2] \tag{14}$$

$$V / W = [v_1, v_2] / [w_1, w_2] = [v_1 / w_2, v_2 / w_1] \tag{15}$$

$$V / h = [v_1, v_2] / h = [v_1 / h, v_2 / h] \tag{16}$$

The multiplication between two fuzzy membership functions using equation (14) is shown in Fig. 3.

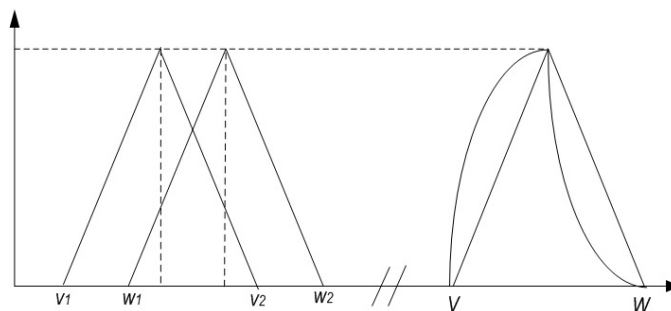


**Fig. 3:** Multiplication of two fuzzy membership function of unavailability.

It should be noted that, multiplication, division, and inversion between two fuzzy membership functions do not give a triangular result Bowles and Pelaez, (1995). Therefore,

**Fuzzy Model of Peak Load and Load Curve:**

Load duration curve and peak load models are the information that needs to be considered in the risk evaluation of a system. This section discusses on a fuzzy model of peak load and probability of load level.

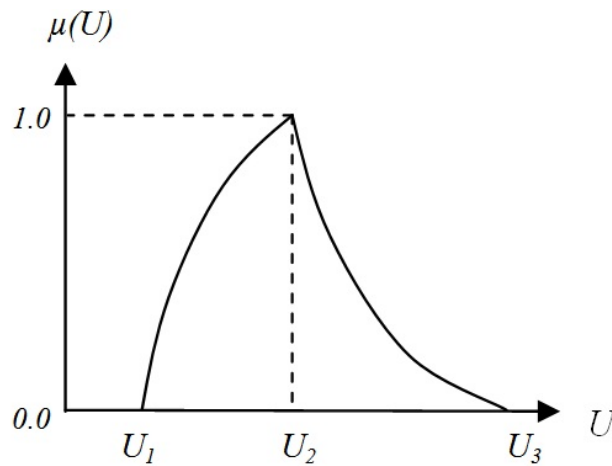


Fig. 4: Membership function of unavailability.

**Fuzzy Model for Peak Load:**

The peak loads are usually forecasted within the range of its upper and lower bounds. This information can be used to construct a triangular membership function for the peak load that is similar to the concept of fuzzy model Li, (2005). Fig. 5 shows an asymmetrical triangle membership function of peak load. The peak load with highest probability ( $L_{peak}$ ) is specified as membership grade 1.0. The upper ( $L_{high}$ ) and lower ( $L_{low}$ ) bounds are specified for the membership grade zero.

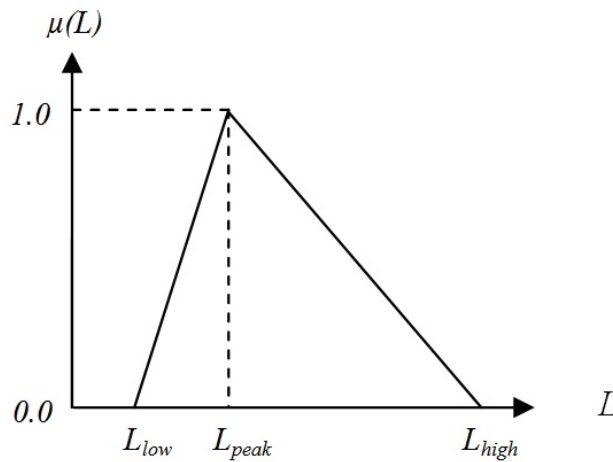


Fig. 5: Membership function of peak load.

**Probabilistic Model for Load Curve:**

A load duration curve is consisting of load profile at different time intervals and it is usually used in the assessment of power system reliability Verdonck *et al.*, (2000). It can be used to determine the probability for every load level. Assume that the load duration curve with  $NT$  hourly load points is divided into nine load levels. The probability for every load level is calculated by,

$$P_i = \frac{NI_i}{NT} \tag{17}$$

where,

$i : 1, 2, \dots, NL.$

$NL$ : number of load levels in the annual load duration.

$NI_i$  : total number of load points located between the  $i^{th}$  level and the next level.

NT : total number of load points.

The probability distribution for every load level can also be expressed as,

$$p \left[ L_i (\text{per unit}) \right] = p_i \quad (i = 1, \dots, NL) \tag{18}$$

where,

$L_i (\text{per unit})$  : estimated per unit load at load level,  $i$

$p_i$  : probability of  $L_i$ .

The methodology used to calculate the load level  $L_i$  is presented in the following procedure. Basically, clustering technique is used to determine the load levels  $L_i$ , (2005). Each load level represents as the mean value of load in a cluster and the procedure is described as follows:

- a) Divide the load duration curve into  $i^{\text{th}}$  cluster.
- b) Select the initial value of cluster mean,  $M_i$ , for every level.

$$M_i = \frac{1}{NI_i} \sum_{k=1}^{NI_i} L_k \tag{19}$$

where,

$L_k$  : hourly peak load.

$k$  : 1, 2, .....,  $NI$ .

- c) Use the value of cluster mean,  $M_i$ , to calculate the distance  $D_{ki}$  for every load point using equation (20).

$$D_{ki} = |M_i - L_k| \tag{20}$$

- d) Regroup all the load points with nearest cluster based on the distance,  $D_{ki}$ , calculated in step c). Then, calculate a new cluster mean for every load level using equation (19).
- e) Repeat steps c) and d) until all cluster means remain unchanged after several iterations.
- f) The per unit value of load at every level is calculated as follows:

$$L_i (\text{per unit}) = \frac{M_i}{L (\text{peak})} \tag{21}$$

where,

$L (\text{peak})$  : peak load in a year.

- g) Calculate the sample standard deviations for every load level using equation (22).

$$\sigma_i = \sqrt{\frac{1}{NI_i - 1} \sum_{k=1}^{NI_i} (L_k - M_i)^2} \tag{22}$$

The standard deviation,  $\sigma_i$ , and  $L_i$  are used to obtain the fuzzy random peak loads at every load level.

**Case 1: Determination of Risk Indices Using Fuzzy Set:**

The information of failure indices and system load represent as the random fuzzy variables that can be used to determine the risk indices. The expected energy not supplied (EENS) and probability load curtailment (PLC) are the risk indices presented in terms of fuzzy membership function. The procedures that used to determine the fuzzy membership of risk indices are described as follows.

- a) Determine the membership functions of failure frequency and repair time for all components. The membership function for both repair time and failure frequency can be obtained as explained in Sections II.A and II.B, respectively.
- b) Calculate the membership functions of unavailability by multiplying both membership functions obtained in a).

$$U = \frac{f \times r}{8760 \text{ hours / year}} \tag{23}$$

- c) Determine the fuzzy membership function of system peak load and the probability distribution model of load level as explained in Section III.
- d) Calculate the inverse fuzzy membership function of peak load,  $\mu^{-1}(L)$ . The fuzzy membership function and inverse fuzzy membership function of peak loads are illustrated in Figure 6 and Figure 7, respectively.

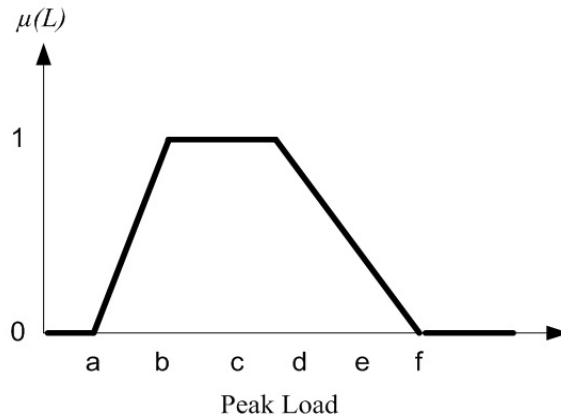


Fig. 6: Fuzzy membership functions of peak load.

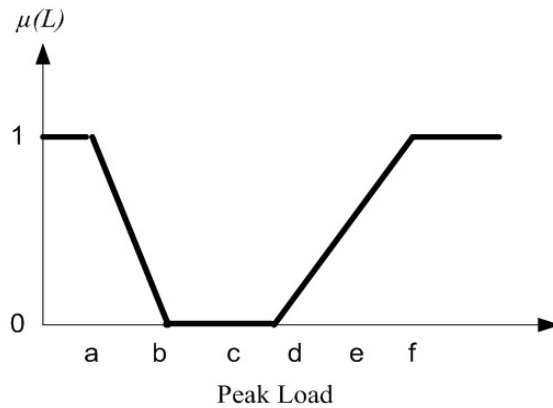


Fig. 7: Inverse fuzzy membership functions of peak load.

- e) Calculate the inverse fuzzy membership function of unavailability for every component,  $j$ ,  $\mu^{-1}(U_j)$
- f) Determine the value of MW load at every level as well as at every grade of inverse fuzzy membership function. This can be obtained by using equation (24).

$$L_i(MW) = L_i(\text{per unit}) \times \mu^{-1}(L) \tag{24}$$

- g) Use the Monte Carlo simulation technique in equation (25) to provide a sample of MW peak load at every grade of inverse fuzzy membership function as well as every load level,  $i$ .

$$L_{im} = X_m c_i + L_i(MW) \tag{25}$$

where,

$X_m$  : uniformly distributed random number between 0 and 1.

- h) Use the Monte Carlo simulation technique in equation (26) to specify the system state of every component.

$$s_j = \begin{cases} 0(\text{up}), & \text{if } R_j > \mu^{-1}(U_j) \\ 1(\text{down}), & \text{if } R_j < \mu^{-1}(U_j) \end{cases} \quad (26)$$

where,

$R_j$  : uniformly distributed random number between 0 and 1.

- i) Calculate the expected energy not supplied (EENS) and the probability of load curtailment (PLC). For every grade of fuzzy membership function, the component states,  $s_j$ , are applied at every variable in the sample of load level,  $i$ , obtained in equation (25). The energy not supplied (ENS) is obtained by referring to the amount of load demand exceeding the generation capacity. For every grade of fuzzy membership function, the expected energy not supplied (EENS) is determined as the average value of ENS at every load level. On the other hand, the load curtailment is performed in order to improve the violation of transmission line limit. This has been explained elaborately in Section V. The probability of load curtailment, PLC, is obtained by referring to the average value of load curtailment at every fuzzy membership grade.
- j) Use equation (27) to calculate the total EENS at every fuzzy membership grade,  $l$ .

$$EENS_l(\text{total}) = \sum_{i=1}^{NL} EENS_l(L_i) \times p_i \quad (27)$$

**Load Curtailment Considering DC Power Flow:**

The generation and transmission line outages may cause to the violations of transmission line. Hence, the load curtailment should be applied in order to avoid the occurrence of overloaded line due to the nuances of generator outage, transmission line outage, generating rescheduling or uncertain load variation. The load is usually curtailed at the industrial, large commercial and utility systems. The operation of the systems is monitored continuously (usually by automated instrumentation) and shutting down certain pre-arranged electric loads or devices when a certain upper threshold of electric usage is reached.

In this paper, the load curtailment was performed at the receiving-end buses that are connected to the overloaded lines. A DC power flow solution is performed to observe the violations of transmission line limit due to the occurrence of component outages and load variation. There will be no load curtailment when the generation capacity exceeds the total load demand and vice versa Shandilya *et al.*, (1993). Then, the risk index of expected energy not supplied is determined by considering the load curtailment.

A DC power flow solution is very similar to a fast decoupled method that used in the AC power flow solution Van Hertem *et al.*, (2005). It offers a linear mathematical solution but less accurate compared to the AC power flow solution. The DC power flow calculation requires the parameters of active power flow and neglecting the voltage magnitude, reactive power and transmission losses (Van Hertem *et al.*, 2005; Overbye *et al.*, 2004). A DC power flow solution does not require any repetitive mathematical calculation as it is happened in the AC power flow solution. Hence, fast computational time of DC power flow solution can be obtained. A DC power flow solution offers simple calculation of power flow by taking into account several assumptions described as follows Li, (2005).

- a) The branch resistance is smaller than the reactance. Therefore,

$$c_{de} \approx \frac{-1}{x_{de}} \quad (28)$$

- b) By assuming that all voltage magnitudes are identical as one per unit. That is,

$$|E_d| = |E_e| = 1 \quad (29)$$

- c) Small voltage angle difference as shown in equation (30).

$$\sin \delta_{de} \approx \delta_d - \delta_e \quad (30)$$

$$\cos \delta_{de} \approx 1.0$$

- d) Ignoring the transformer tap changer. Then,

$$c_{d0} = c_{e0} \approx 0 \tag{31}$$

Base on the above mentioned assumptions, a real power flow can be calculated by using equation (32).

$$P_{de} = \frac{\delta_d - \delta_e}{x_{de}} \tag{32}$$

Thus, a real power injection at every bus can be obtained by using equation (33).

$$P_d = \sum_{e \in R_d} P_{de} = C'_{dd} \delta_d + \sum_{e \in R_d} C'_{de} \delta_e \tag{33}$$

where,

$P_{de}$  : power flow at transmission line between bus  $d$  and  $e$ .

$\delta_d$  : voltage angle at bus  $d$ .

$\delta_e$  : voltage angle at bus  $e$ .

$C'$  : bus susceptance matrix.

**Bootstrapping:**

Bootstrapping is a computationally intensive technique that used for making inferences. It is different from the traditional parametric approach such as Monte Carlo technique in which it employs large number of repetitive computations for re-sampling without strong distributional assumptions and analytical formulation (Bradley and Tibshirani, 1994). The bootstrap technique is normally done by drawing a large number of samples based upon original data in order to estimate the statistic of interest. Although each sample has the same number of elements as the original however, each sample could have some original data points represented in it more than once and some are not represented at all. The main advantage of bootstrap technique is that it can provide estimation in situations where mathematical solutions are not possible (Bradley and Tibshirani, 1994).

In this section, the bootstrap technique that used for clustering the load is first explained and then followed by the explanation of bootstrap technique that used to specify the system states for every component.

**Bootstrap Samples of Peak Loads:**

The bootstrap technique that used to determine several samples of MW peak load is described in the following procedures.

- a) Divide the load duration curve into  $i^{\text{th}}$  load level. Every load level consisting of  $k^{\text{th}}$  number of load points,  $L_k$ .
- b) Select load level  $i$ .
- c) Use a random number generator to draw a random sample of  $k$  values, and replace the measured sample data points,  $L_k$ , with the bootstrap sample,  $L_k^*$ .
- d) Repeat step c) in order to obtain a total number,  $B$  of bootstrap samples,  $L_{k,b}^*$ , where  $b=1,2,3,\dots,B$ .
- e) Determine the nearest neighbor samples of  $L_{k,b}^*$  using (34).

$$D_{k,b} = \left| L_k - L_{k,b}^* \right| \tag{34}$$

- f) Regroup all the samples of  $L_{k,b}^*$  with nearest cluster. The nearest cluster of samples  $L_{k,b}^*$  are obtained based on the average sample value of  $D_{k,b}$ .
- g) Compute the average value of every bootstrap sample by using (35).

$$M_b = \frac{1}{Nr} \sum_{r=1}^{Nr} L_{k,b}^* \tag{35}$$

where,

$Nr$  : total number of bootstrap samples with nearest cluster.

- h) Repeat steps e), f) and g) until the average value of  $M_b$  remain unchanged after several iterations.
- i) Collect the  $L_{k,b}^*$  with nearest cluster for load level  $i$ .
- j) Calculate the probability,  $p_i$ , for every load level,  $i$ , calculated by using equation (17).
- k) Go to step b) to determine the  $L_{k,b}^*$  with nearest cluster for the next level  $i$ .
- l) Stop the procedure when  $i=NL$ .

**Determination of System States Using Bootstrap Technique:**

This section discusses on the determination of system states using the bootstrap technique. Historically, the occurrence of major power outage and blackouts were associated with the system state of dependent failure event. The following procedure presents the determination of system states using the bootstrap technique.

- a) Select load level  $i$ .
- b) Specify a sample of system or components status,  $s$ , consisting of two component outages, 0, and the rest are in-service, 1. The outage of two components is selected randomly.
- c) Use a random number generator to draw a random sample of  $j$  values, and replace the actual sample of  $s_j$  with the non-parametric bootstrap sample of  $s_{j,b}^*$ . Where  $j$  is the number of component.
- d) Repeat step (b) in order to obtain bootstrap samples of  $s_{j,b}^*$ .
- e) Discard any sample comprising of more than two component outages. Retain any sample with one, (N-1), and two, (N-2), components, and proceed to the next procedure.
- f) Select any bootstrap samples of  $s_{j,b}^*$  which brings to  $B=Nr$ . The  $Nr$  is specified at load level  $i$  as explained in Section VI.A.
- g) Go to step a) to determine the  $s_{j,b}^*$  with  $B=Nr$  for the next load level  $i$ .
- h) Stop the procedure when  $i=NL$ .

The above-mentioned procedure elucidates that the bootstrap samples  $s_{j,b}^*$  with  $B=Nr$  are determined for every load level,  $i$ .

**Case 2: Determination of Risk Indices Using Bootstrap Technique:**

This section present the risk assessments of expected energy not supplied (EENS) and probability of load curtailment (PLC) that takes into account the bootstrap samples of peak loads and system states. This methodology is explained in the following procedure.

- a) Use the bootstrap technique to determine several samples of peak loads,  $L_{k,b}^*$ , with nearest cluster for every load level  $i$ . This has been explained elaborately in Section VI.A.
- b) Use the bootstrap technique to specify several samples of system states,  $s_{j,b}^*$  with  $B=Nr$  for every load level  $i$ .
- c) Calculate the expected energy not supplied (EENS) and probability of load curtailment (PLC). For every bootstrap sample, the component states,  $s_{j,b}^*$ , are applied at every variable of sample  $L_k^*$  for every load level,  $i$ . The energy not supplied (ENS) is obtained by referring to the amount of load demand exceeding the generation capacity.
- d) Determine the expected energy not supplied (EENS) for every bootstrap sample based on the average value of ENS as given in equation (36).

$$EENS_b = \frac{1}{NL} \sum_{i=1}^{NL} \left[ ENS_i \left( L_{k,b}^* \right) \times p_i \right] \tag{36}$$

The bootstrap sample of  $EENS_b$  can be selected based on the confidence interval of the mean of bootstrap sample. The desired  $(1 - \alpha) \cdot 100\%$  bootstrap confidence interval of uncertainty is between the range of

$EENS_{b=q_1}$  and  $EENS_{b=q_2}$ , where  $q_1 = (B\alpha / 2)$  and  $q_2 = B - q_1 + 1$ . Note that for 95% bootstrap

confidence interval,  $\alpha=0.05$ . In which,  $\alpha$  is a degree of confidence. On the other hand, the load curtailment is performed in order to improve the violation of transmission line limit. This has been explained elaborately in Section V. The probability of load curtailment, PLC, for every bootstrap sample is obtained by referring to the average value of load curtailment at every bootstrap sample and it is given in equation (37).

$$PLC_b = \frac{1}{NL} \sum_{i=1}^{NL} LC_i \left( L_{k,b}^* \right) \tag{37}$$

where,

$LC$  : the amount of load curtailment.

The bootstrap sample of  $PLC_b$  can also be selected at a particular uncertainty of bootstrap confidence interval. The above-mentioned concept is used to select the bootstrap samples of  $PLC_{b=q_1}$  and  $PLC_{b=q_2}$ .

The bootstrap technique has the advantage of elucidating the result of system risk at every uncertainty of bootstrap confidence interval. This may assist the system operator towards assessing the system risk at worst

condition selected at higher bootstrap confidence interval. On the other hand, the bootstrap technique is superior to fuzzy set in conjunction to its simplicity in producing the uncertainties of system states and peak load conditions for a power system risk assessment.

***Case 3: Determination of Risk Indices Considering Bootstrap Samples of Peak Loads and System States based Fuzzy Set:***

This section discusses on the combined methodology of bootstrap technique and fuzzy set that used to determine the risk indices. Conceptually, the bootstrap technique is used to provide several samples of peak loads and the fuzzy set is used to specify system state of every component. The methodology is discussed as follows.

- a) Use the fuzzy set to determine the system states,  $s_j$ . This refer to steps a), b), e) and h) given in Section IV.
- b) Determine the samples of peak loads using bootstrap technique as explained in Section VI. Use the bootstrap technique to determine several samples of peak loads,  $L_{k,b}^*$ , with nearest cluster for every load level,  $i$ . This has been explained elaborately in Section VI.A.
- c) Perform step c) and d) in Section VII to determine the  $EENS_b$  and the  $PLC_b$  at a particular uncertainty of bootstrap confidence interval.

***Case 4: Determination of Risk Indices Considering Peak Loads Samples based Fuzzy Set and System States based Bootstrap Technique:***

In this section, the bootstrap technique is used to specify the system states while the fuzzy set is used to sample the peak loads. The methodology is explained as follows.

- a) Use the bootstrap technique to specify the system states,  $s_{j,b}^*$ , at every load level,  $i$ . This has been explained elaborately in Section VI.B. In this case, the number of bootstrap sample,  $b$ , is set equivalent to the number of membership grade,  $l$ .
- b) Use the fuzzy set to provide a sample of MW peak load at every grade of inverse fuzzy membership function as well as every load level,  $L_{im}$ . This refer to steps c), d), f) and g) given in Section IV.
- c) Execute steps i) and j) in Section IV to determine the  $EENS_l(\text{total})$  and  $PLC_l(\text{total})$ .

**RESULTS AND DISCUSSION**

The presented method is validated on the 24-bus IEEE RTS as shown in Figure 8. The system consists of three areas. Area 1 and area 2 are interconnected by tie-lines 21–22, 17–22, 19–20 and 11–14. There are 5 tie-lines connecting between area 3 and area 2 which are lines 3–9, 4–9, 1–5, 2–6 and 7–8, and area 1 and area 3 are interconnected by tie-line 3–24. The total load for the system is 2850 MW and the generation capacity is 3405 MW. The generation system contain of 32 units ranging from 12MW to 400MW. The presented methods are used to perform the risk assessment of the power system that takes into account the hourly peak loads in the year 2002.

The results of risk indices can be classified into four main cases as described briefly in the following list. In Case 1, the risk assessment based fuzzy set was developed by [26]. Therefore, it is used as a benchmark for comparing the result of risk indices determined based on Case 2, Case 3 and Case 4.

- a) *Case 1:* Risk assessment using fuzzy set.
- b) *Case 2:* Risk assessment using bootstrap technique.
- c) *Case 3:* Risk assessment considering bootstrap samples of peak loads and system states based fuzzy set.
- d) *Case 4:* Risk assessment considering peak loads samples based fuzzy set and system states based bootstrap technique.

***Case 1: Risk Assessment Using Fuzzy Set:***

In this section, the risk indices of expected energy not supplied (EENS) and probability of load curtailment (PLC) are determined by using the fuzzy set technique. The membership functions for both  $EENS_l(\text{total})$  and  $PLC_l(\text{total})$  are shown in Fig. 9 and Fig. 10, respectively. It is obvious that the membership functions of  $EENS_l(\text{total})$  and  $PLC_l(\text{total})$  are asymmetric since the upper bound is larger than the lower bound. This indicates that the system is stable since the  $EENS_l(\text{total})$  of 883.56 MW occurred close to the lowest  $EENS_l(\text{total})$  of 646.18 MW and it is shown in Fig. 9. The highest  $EENS_l(\text{total})$  is 1419.8 MW. The  $EENS_l(\text{total})$  at membership grade 1 indicates that the system is frequently experiencing the 883.56 MW of

energy not supplied to the customers. The stability of the system can also be proven by referring to the probability of load curtailment (PLC) shown in Fig. 10. The system can be classified as stable referring to  $PLC_i(\text{total})$  value of 498.12 MWh/year that is located close to the lowest  $PLC_i(\text{total})$  of 182.22 MWh/year. The highest  $PLC_i(\text{total})$  is 1214.12 MWh/year. The  $PLC_i(\text{total})$  at membership grade 1 indicates that the system is frequently experiencing the 498.12 MWh/year of load curtailment. The graph shows that when both uncertainty of load variations and system component outage parameters are considered in the risk assessment, their combined impacts on the risk indices are not a simple linear superposition. The risk indices obtained from the presented technique consider the impacts of both randomness and fuzziness of input data.

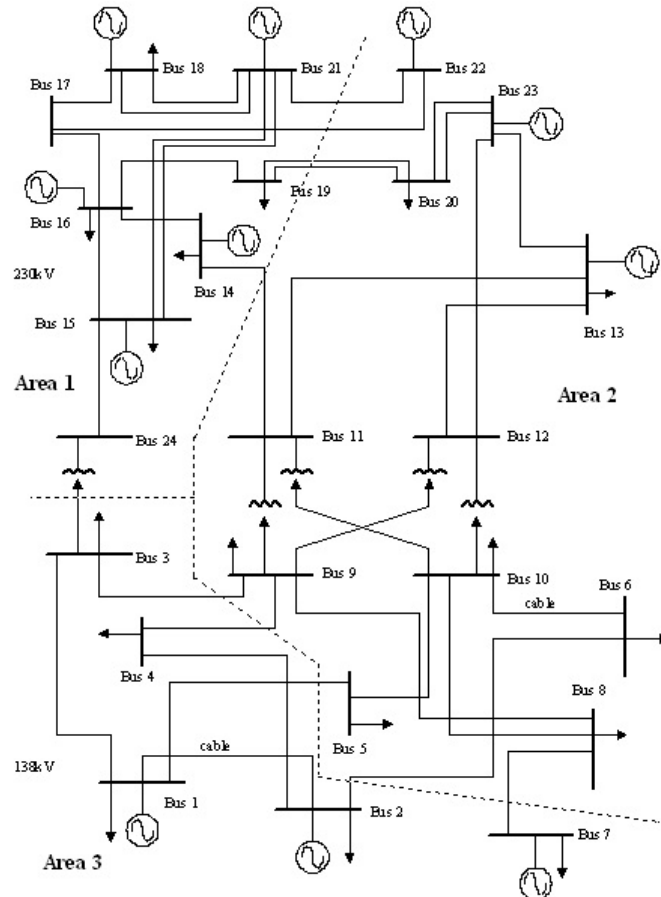


Fig. 8: 24-bus IEEE Reliability Test System.

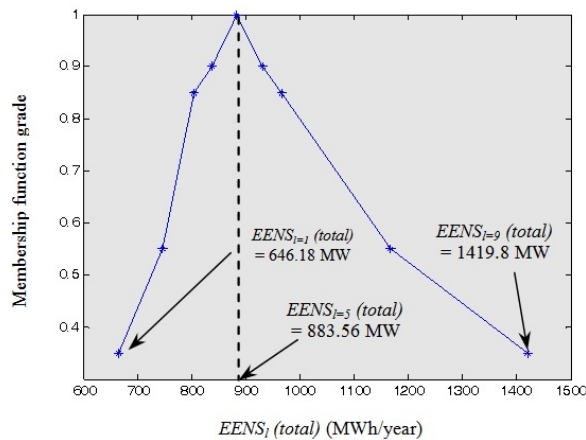


Fig. 9: Membership function  $EENS_i \# (\text{total})$ .

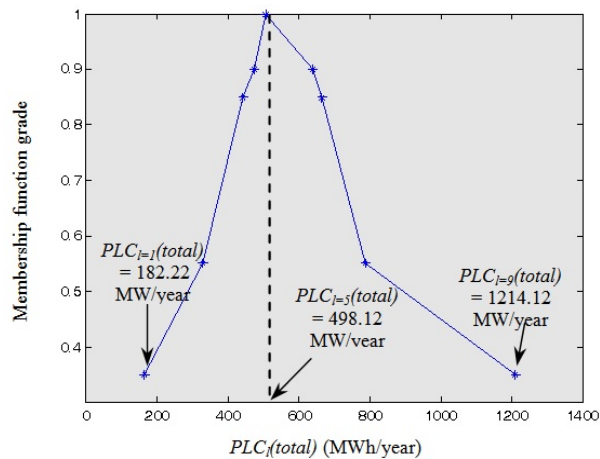


Fig. 10: Membership function of PLC1 # (total).

**Case 2: Risk Assessment Using Bootstrap Technique:**

In this section, the results of risk indices are obtained based on the samples of peak loads and system states determined by using the bootstrap technique. The steps taken by the bootstrap technique in determining the risk indices has been explained elaborately in Section VII. It has the advantage in providing several samples of peak load with nearest cluster,  $L_{k,b}^*$ , for every load level,  $i$ . This has been discussed thoroughly in Section VI.A.

Fig. 11(a)-11(i) presents the comparison between the results of  $L_{im}$  and  $L_{k,b}^*$  determined by the fuzzy set and bootstrap technique, respectively. The determination of  $L_{im}$  has been explained elaborately in steps c), d), f) and g) of Section IV. The results of  $L_{im}$  is depicted in terms of fuzzy membership function grade whereas, the normal cumulative distribution function (CDF) is used to represents the  $L_{k,b}^*$ . Consecutively, for impartial comparison, the  $L_{im}$  is generated up to  $m=2000$  samples which are similar to the total number of bootstrap samples,  $B$ .

In general, a fuzzy membership function grade provides similar information as the CDF. For instance, the value which occurs most frequently represents as the mean value of fuzzy membership function grade. Wherein, the value which is most frequently occurred is indicated at the average or 50% probability of CDF. For both of the CDF and fuzzy membership function grade, the upper and lower ends represent as the highest and lowest risks of a system, respectively.

In Fig. 11(a)-11(i), significant information of uncertainty can be obtained from a large abscissa of CDF determined by the bootstrap technique. This is contrary to the fuzzy set wherein a narrow abscissa of fuzzy membership function grade provides less information of uncertainty for risk assessment. Therefore, it is important to use the bootstrap technique for evaluating the risk at every significant level of uncertainty.

On the other side, the bootstrap technique can be used in providing accurate risk assessment of a power system. This is proven by referring to CDF at 0% of bootstrap confidence interval and it is located at the centre of abscissa shown in Fig. 11(a)-11(i). The CDF located at 0% of bootstrap confidence interval represents as the CDF for inherent or actual value of peak loads. This means that there is no uncertainty in the inherent or actual value of peak loads. By referring to the CDF at 0% of bootstrap confidence interval, the lower end, mean, and upper end of CDF yields to relatively similar value of peak loads compared to the lower end, mean, and upper end of fuzzy membership function grade, respectively. For example, it is observed in Fig. 11(a).ii that the lower end, mean, and upper end of  $L_{k,b}^*$  are 535.1 MW, 926.8 MW, and 1423 MW, respectively. This is relatively similar to the lower end, mean, and upper end of  $L_{im}$  which are 682 MW, 891.4 MW, and 1420 MW, respectively as shown in Fig. 11(a).i. This shows that the bootstrap technique can be used in providing accurate result of risk assessment.

Nevertheless, the bootstrap technique has the advantage in assessing the risk assessment at every level of uncertainty. This is important to a system planner so that they could assess the risk at several levels of uncertainty. In Fig. 11(a)-11(i), upper and lower CDFs with larger uncertainty can be selected by increasing the percentage of bootstrap confidence interval.

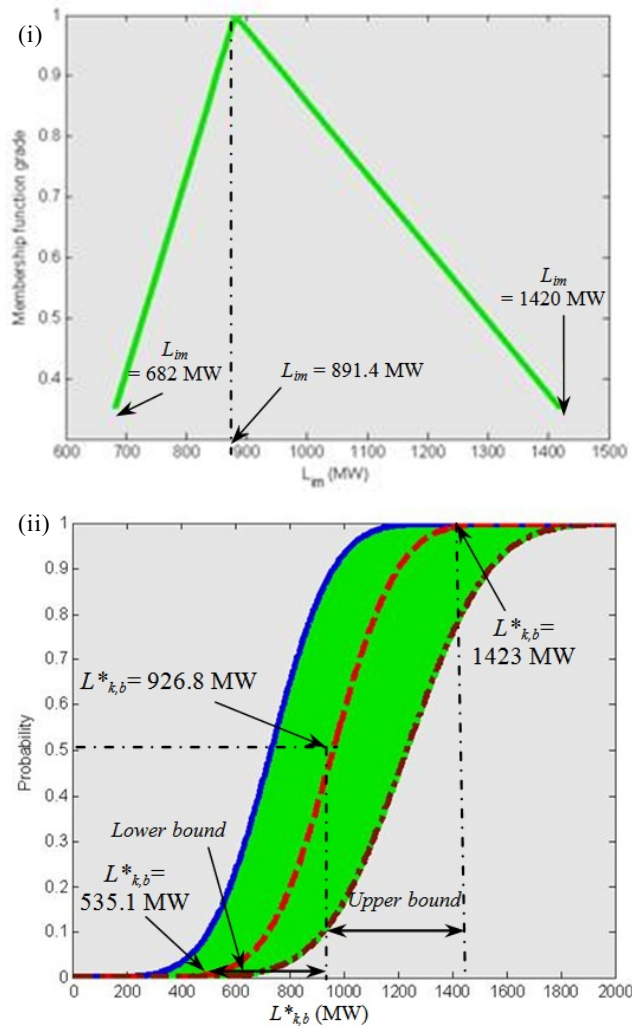
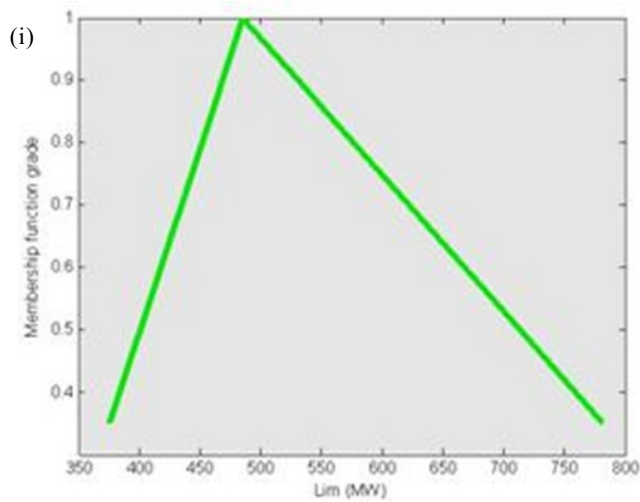


Fig. 11(a): Fuzzy triangle (i) and normal CDF (ii) of load level 1.



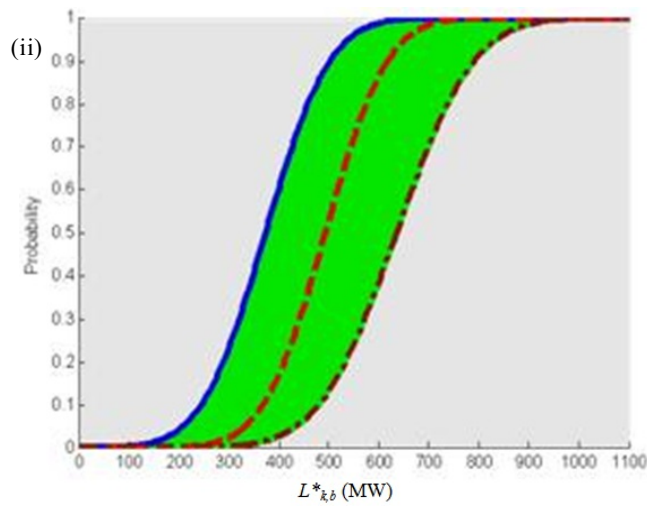


Fig. 11(b): Fuzzy triangle (i) and normal CDF (ii) of load level 2.

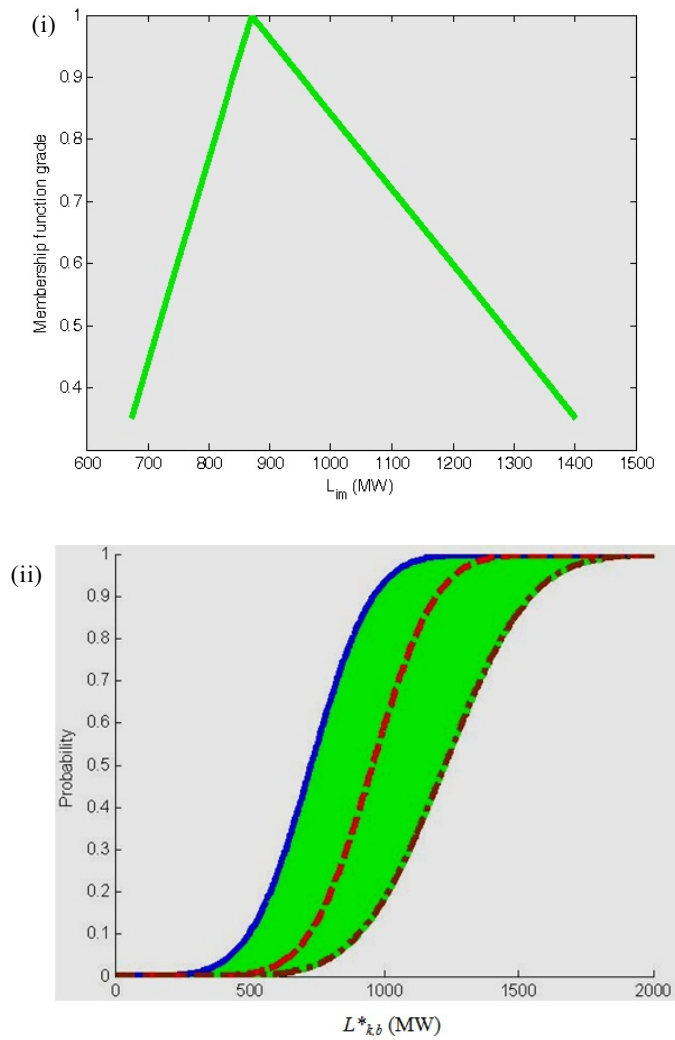


Fig. 11(c): Fuzzy triangle (i) and normal CDF (ii) of load level 3.

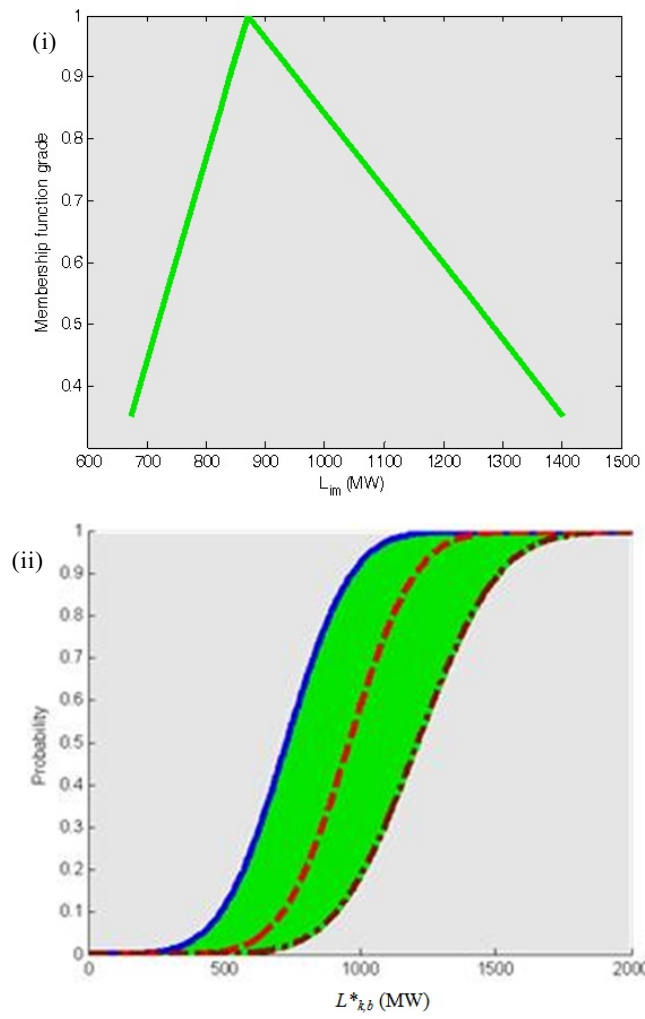
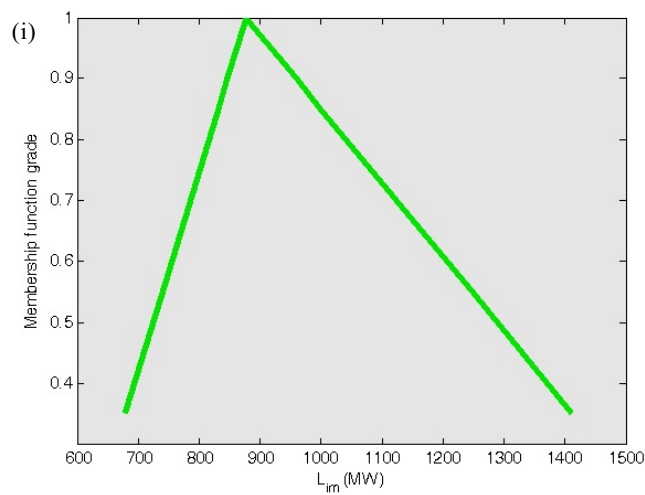


Fig. 11(d): Fuzzy triangle (i) and normal CDF (ii) of load level 4.



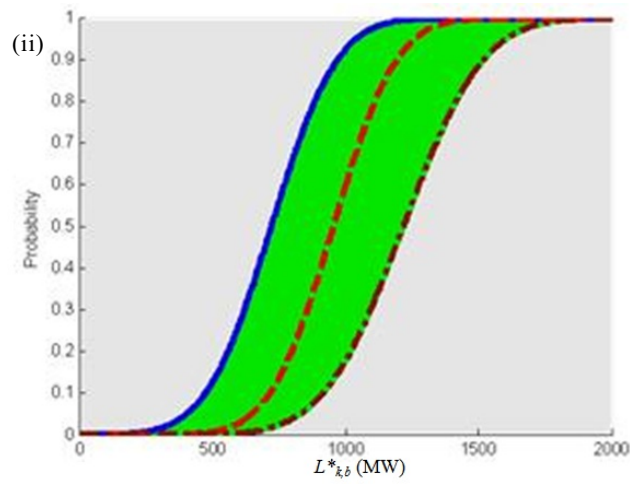


Fig. 11(e): Fuzzy triangle (i) and normal CDF (ii) of load level 5.

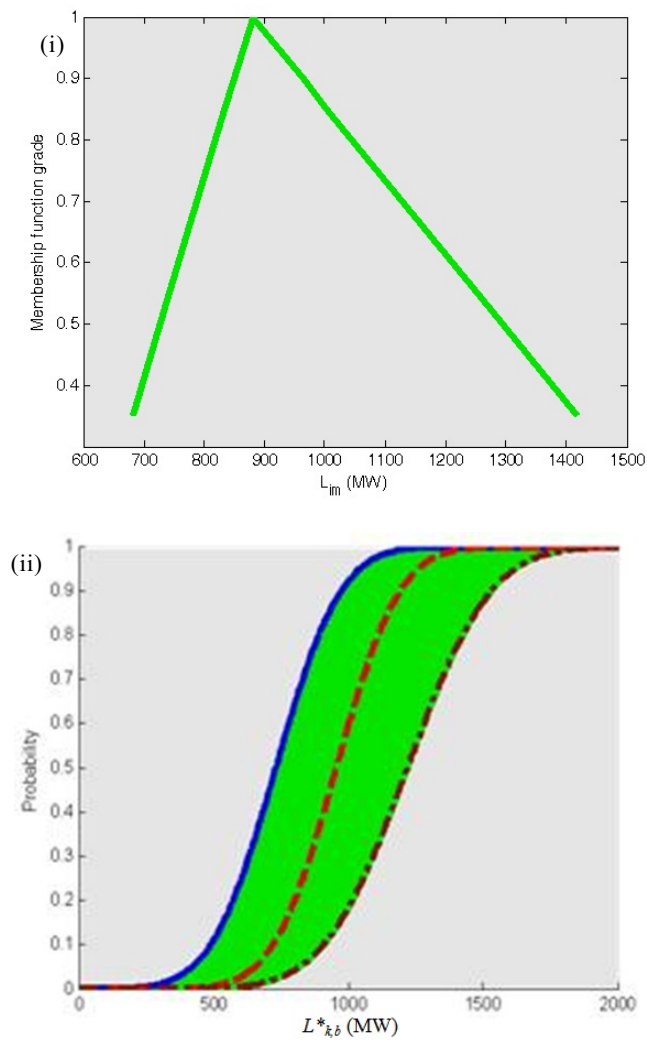
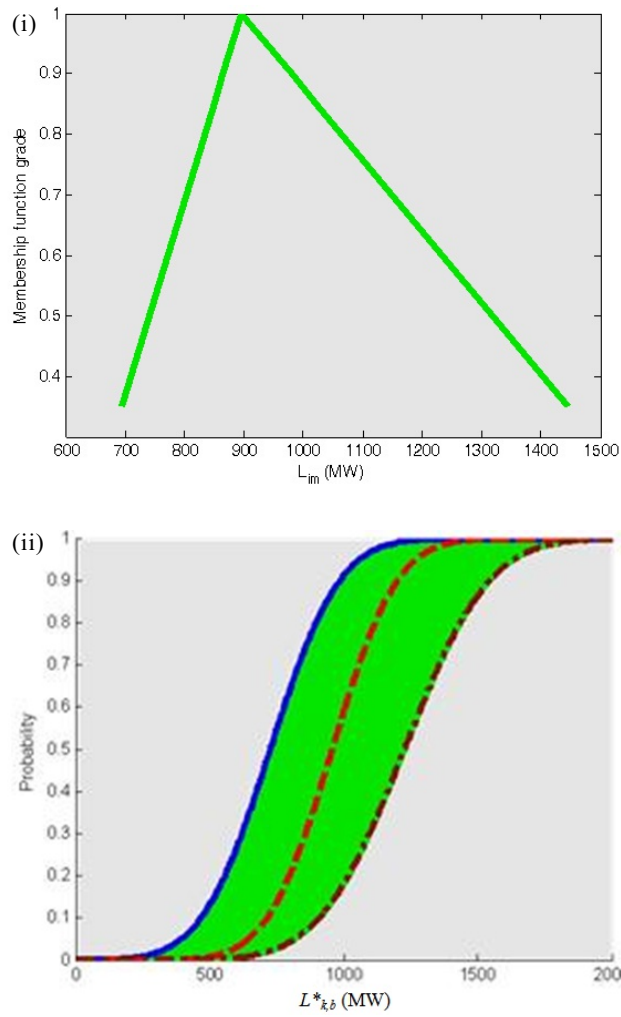
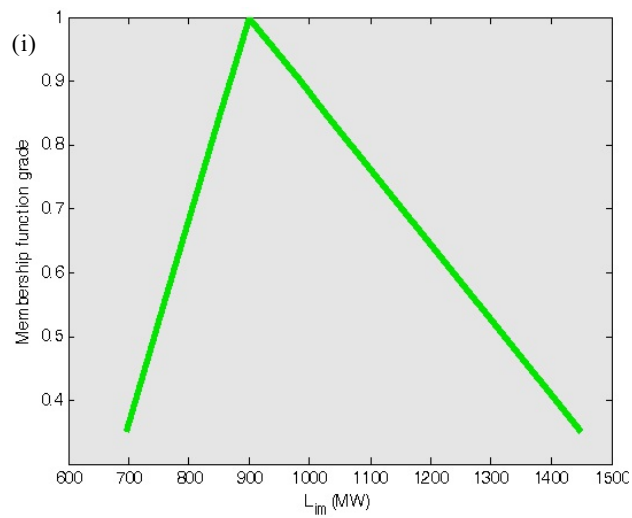


Fig. 11(f): Fuzzy triangle (i) and normal CDF (ii) of load level 6.



**Fig. 11(g):** Fuzzy triangle (i) and normal CDF (ii) of load level 7.



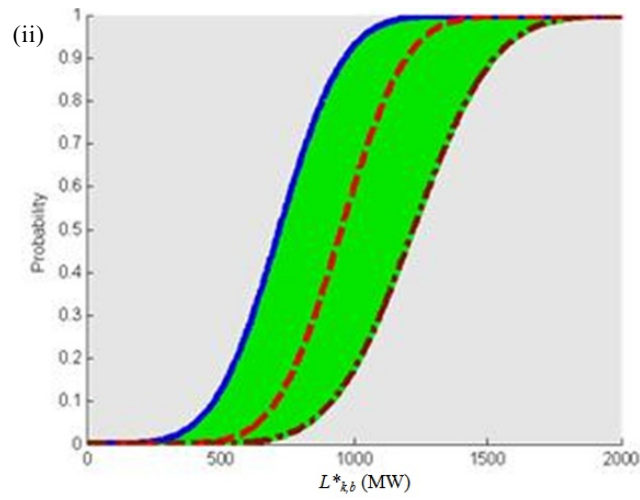


Fig. 11(h): Fuzzy triangle (i) and normal CDF (ii) of load level 8

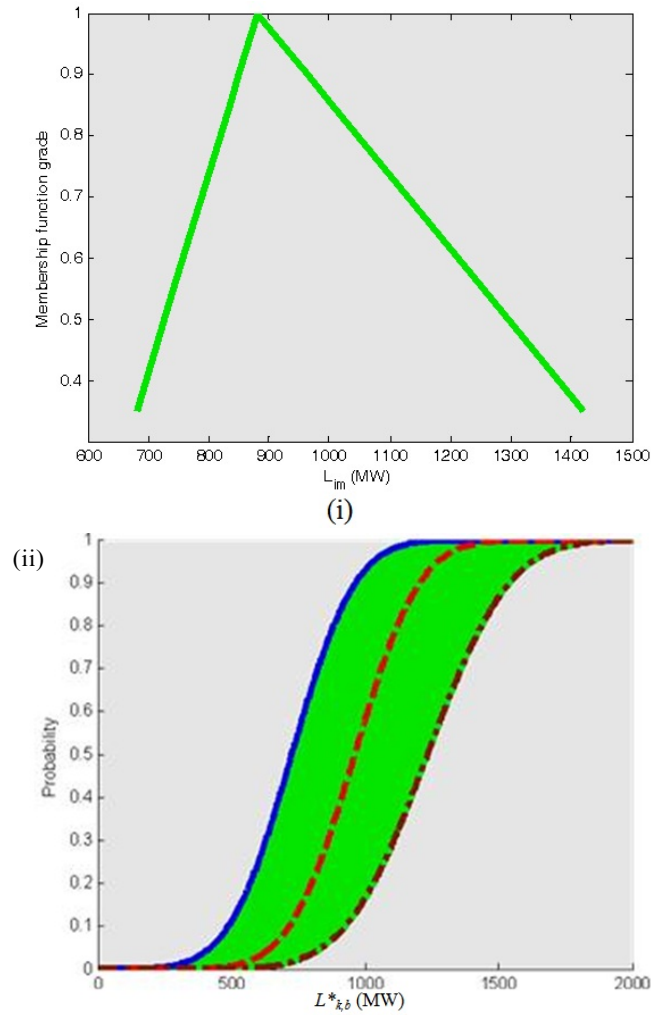


Fig. 11(i): Fuzzy triangle (i) and normal CDF (ii) of load level 9.

The nearest cluster of  $L_{k,b}^*$  at every load level  $i$  and several bootstrap samples of system states,  $s_{j,b}^*$  are then used to determine the risk indices of  $EENS_b$  and  $PLC_b$ . This has been discussed elaborately in Section VII. Fig. 12 and Fig.13 represent the abscissa of CDF for  $EENS_b$  and  $PLC_b$  determined by using the bootstrap technique, respectively. In Fig. 12, by referring only to the CDF of  $EENS_b$  selected at the 0% of bootstrap confidence interval, the bootstrap technique gives the upper end, mean and lower end values of 301.9 MW, 839.37 MW and 1651.52 MW respectively. This is relatively similar to the upper end, mean and lower end values of 646.18 MW, 883.56 MW and 1419.8 MW respectively for the  $EENS_{i(\text{total})}$  determined by the fuzzy set and this is shown in Fig. 9. This shows that the bootstrap technique can be used to determine accurate values of EENS which is relatively similar to the results of EENS determined by using the fuzzy set. Furthermore,  $EENS_b = 839.37$  MW is the mean value of CDF located near to the lower end of CDF that is 301.9 MW. However, the mean value of CDF with  $EENS_b = 839.37$  MW is located far from the upper end of CDF that is  $EENS_b = 1651.52$  MW. This indicate that the system is stable since the mean  $EENS_b$  of 839.37 MW occurred close to the lower end  $EENS_b$  of 301.9 MW.

The bootstrap technique has the advantage in providing the  $EENS_b$  with large uncertainty selected at a certain percentage of bootstrap confidence interval. For instance, by referring to Fig. 12,  $EENS_{b=q_1}$  and  $EENS_{b=q_2}$  are the lower bound and upper bound of CDFs with large uncertainty selected at the 99.5% of bootstrap confidence interval, respectively. The most severe condition of the power system can be obtained by referring to the upper end of  $EENS_{b=q_2}$  that is 1150 MW and the lower end of  $EENS_{b=q_1}$  that is 751.2 MW represents as the safest condition of the power system.

Moreover, the power system risk can also be measured based on the probability of load curtailment (PLC) determined by using the bootstrap technique. Fig. 13 shows the abscissa of CDF for  $PLC_b$  determined by using the bootstrap technique. The result of  $PLC_b$  brings to the same discussion for the result of  $EENS_b$ . It is observed that the  $PLC_b = 627.4$  MW/year is the mean value of CDF located near to the lower end of CDF that is  $PLC_b = 300$  MW/year, compared to the upper end of CDF that is  $PLC_b = 971.43$  MW/year. Therefore, the system is said to be stable as the mean  $PLC_b$  of 627.4 MW/year is located close to the lower end  $PLC_b$  of 300 MW/year. On the other hand, by referring to 99.5% of bootstrap confidence interval, the most severe condition of the power system can be obtained based on the upper end of  $PLC_{b=q_2}$  that is 733.3 MW/year and the lower end of  $PLC_{b=q_1}$  that is 116.7 MW/year represents as the safest condition of the power system.

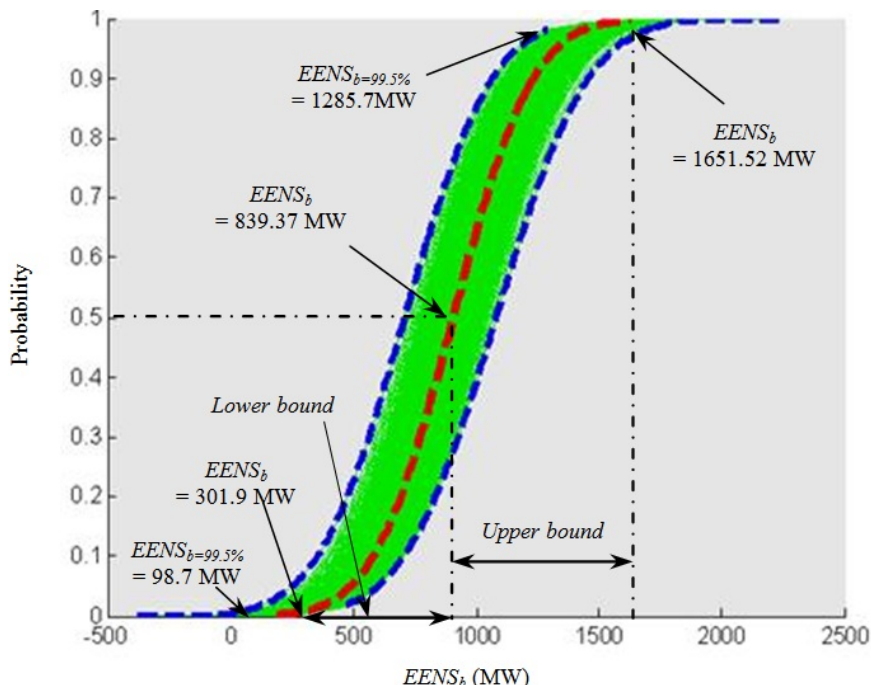


Fig. 12: Normal CDF of  $EENS_b$ .

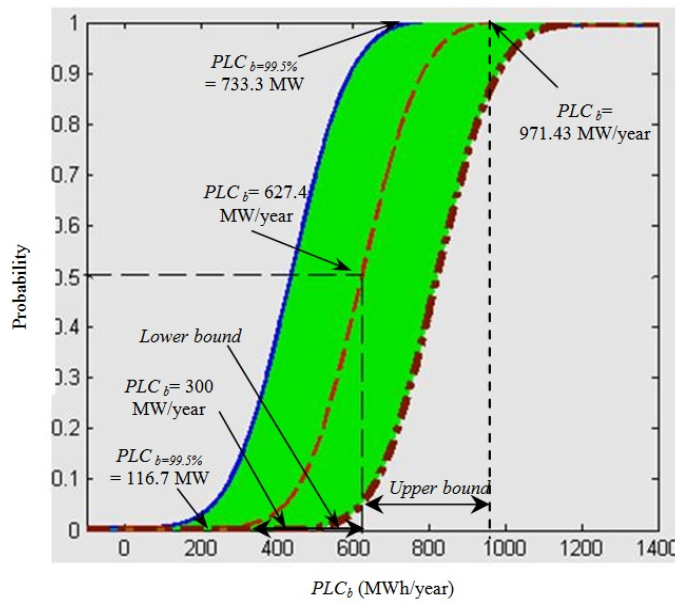


Fig. 13: Normal CDF of  $PLC_b$ .

**Case 3: Risk Assessment Considering Bootstrap Samples of Peak Loads and System States based Fuzzy Set:**

This section presents the results of  $EENS_b$  and  $PLC_b$  obtained by using the combined methods of bootstrap technique and fuzzy set. The bootstrap technique is used to sample the peak loads while the fuzzy set is used to specify the system state. The methodology has been explained thoroughly in Section X. The results of  $EENS_b$  and  $PLC_b$  are depicted in Fig. 14 and Fig. 15, respectively. The graphs are represented in the form of abscissa of CDF. In Fig. 14, by referring only to the CDF of  $EENS_b$ , the bootstrap technique gives the upper end, mean and lower end values of 349.4 MW, 865.5 MW and 1422 MW respectively. This is relatively similar to the upper end, mean and lower end values of 646.18 MW, 883.56 MW and 1419.8 MW respectively for the  $EENS_b$ (total) determined by the fuzzy set shown in Fig. 9. Hence, the system is in stable condition since the mean value of  $EENS_b$  occurs near to the lower end. This also can be proven by referring to  $PLC_b$  as depicted in Fig. 14. The mean value of 586.7 MW/year occurs near to the lower end value, 98.2 MW/year. The highest  $PLC_b$  value is 1209 MW/year. The result for  $EENS_b$  and  $PLC_b$  for Case 3 is relatively similar to the Case 1. It can be concluded that the combined methods of bootstrap technique and fuzzy set used in Case 3 is an effective method for risk assessment as it is relatively similar to the results obtained in Case 1.

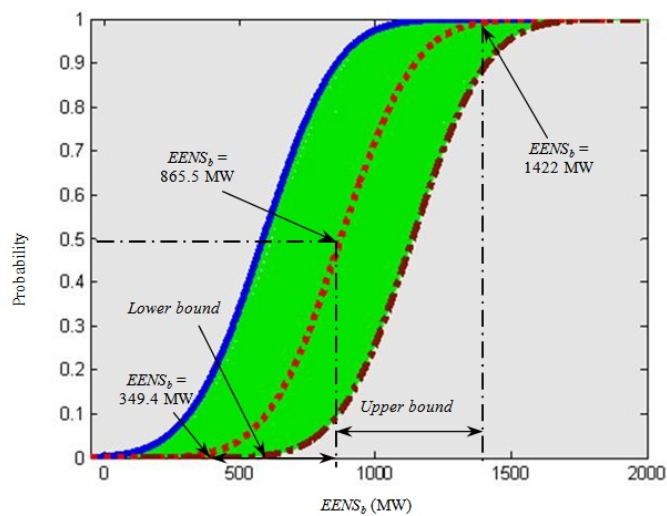


Fig. 14: Normal CDF of  $EENS_b$ .

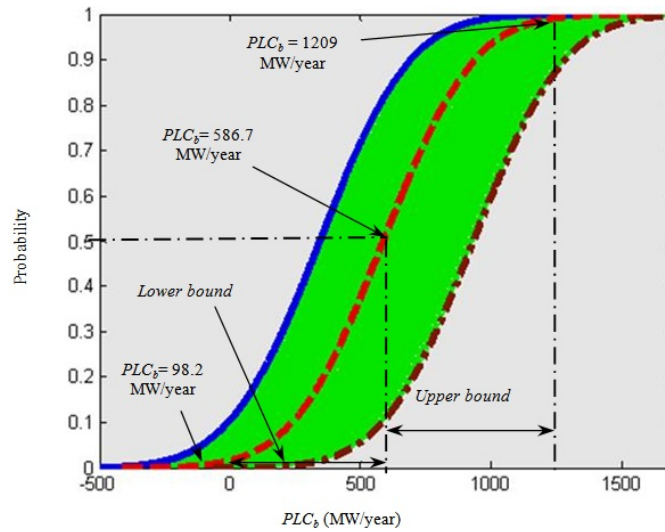


Fig. 15: Normal CDF of  $PLC_b$ .

**Case 4 : Risk Assessment Considering Peak Loads Samples based Fuzzy Set and System States based Bootstrap Technique:**

This section presents the results of  $EENS_i(\text{total})$  and  $PLC_i(\text{total})$  that takes into account the system states and peak loads determined by the bootstrap technique and fuzzy set, respectively. The methodology has been explained in Section IX. The results of  $EENS_i(\text{total})$  and  $PLC_i(\text{total})$  are presented in fuzzy membership function. It is obvious that the mean  $EENS_i(\text{total})$  of 757.8 MW is located near to the lower end of  $EENS_i(\text{total})$  that is 559.2 MW. The upper end of  $EENS_i(\text{total})$  is 1294 MW. Hence, the power system is stable due to the fact that the mean  $EENS_i(\text{total})$  is located near to the lower end of  $EENS_i(\text{total})$ . By comparing the results depicted in Fig. 16 and 9, Case 4 provides the fuzzy membership function of  $EENS_i(\text{total})$  that is relatively similar to the Case 1. However, this is different to the results of  $PLC_i(\text{total})$ . In Fig. 17, the power system is believed to be unstable since the mean of  $PLC_i(\text{total})$  skewed towards the upper end of  $PLC_i(\text{total})$  and it is referring to Case 4. This is contrary to Case 1 in which the mean of  $PLC_i(\text{total})$  is skewed towards the lower end of  $PLC_i(\text{total})$  as depicted in Fig. 10. It can be seen that the bootstrap technique and fuzzy set used in Case 4 is not an effective method for risk assessment as it is contradicting to the results of  $PLC_i(\text{total})$  provided in Case 1.

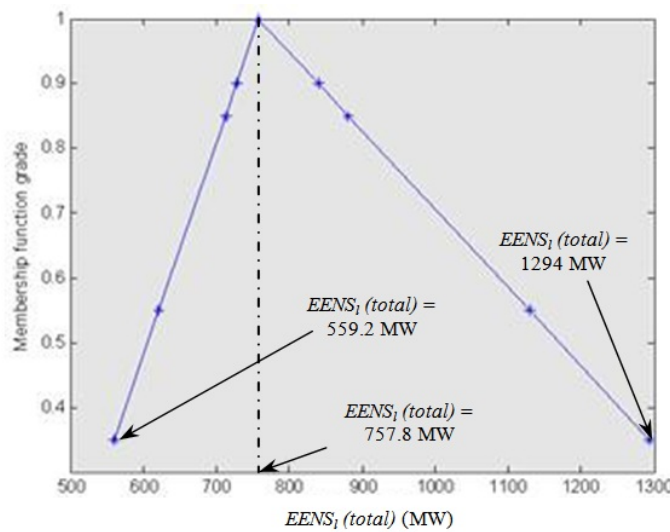
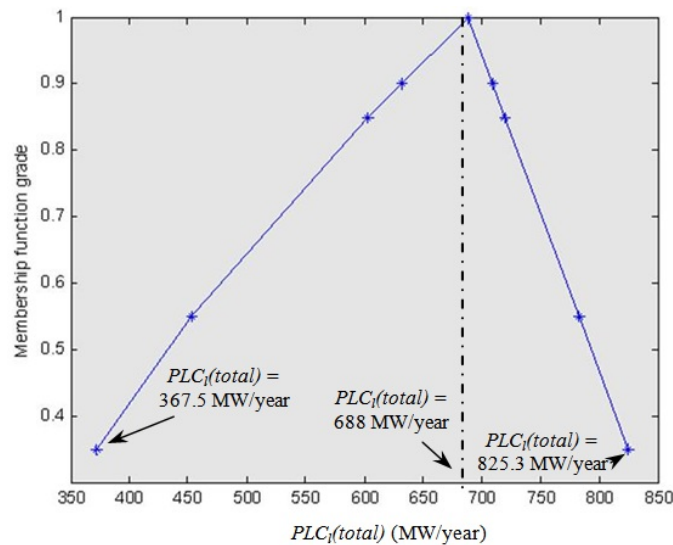


Fig. 16: Membership function of  $EENS_i(\text{total})$ .



**Fig. 17:** Membership function of  $PLC_I(total)$ .

**Conclusion:**

This paper has presented the methods in evaluating the power system risk by taking into account the system component outage parameters and the uncertainty of unavailable load variations. The methods that have been used are such as the fuzzy set, bootstrap technique and; the combined fuzzy set and bootstrap technique. The bootstrap technique is observed to be the simplest way to perform risk assessment of a power system compared to the fuzzy set. Besides providing simplest way in assessing the risk, bootstrap technique also has the advantage in assessing the risk assessment at every level of uncertainty. This is important to a system planner as they could assess the risk at several levels of uncertainty. Comparative studies between fuzzy set, bootstrap and; the combined fuzzy set and bootstrap have been made to evaluate the effectiveness of the presented method in risk assessment. The results show that the bootstrap technique can be used in providing accurate result of risk assessment. On the other hand, the results show that the bootstrap technique provides realistic information of uncertainty as compared to the fuzzy set.

**ACKNOWLEDGEMENT**

This work was done under the auspices of the Ministry of Science, Technology and Innovations (MOSTI), Malaysia and Research Management Institute (RMI), Universiti Teknologi MARA, Malaysia.

**REFERENCES**

“KL, Selangor, Putrajaya, Johor Hit by Major Blackout, 2005. ” The Star, January 13.  
 Information on the electric system blackouts in North America was obtained from the North American Electric Reliability Council website. [Online]. Available: <http://www.nerc.com/filez/blackout.html>  
 Li, W., 2005. Risk Assessment of Power Systems: Models, Methods, and Applications. New York: IEEE Press/Wiley.  
 Billinton, R., and W. Li, 1994. Reliability Assessment of Electric Power Systems Using Monte Carlo Methods. New York: Plenum.  
 IEEE Tutorial Course Text, 2005. Electric Delivery System Reliability Evaluation, 05TP175.  
 Schilling, M.T., 1990. Bibliography on power system probabilistic analysis (1962–88). IEEE Trans. Power Syst., 5(1): 1-11.  
 Allan, R.N., R. Billinton, A.M. Breipohl, and C.H. Grigg, 1999. Bibliography on the application of probability methods in power system reliability evaluation: 1992–1996. IEEE Trans. Power Syst., 14(1): 51-57.  
 Billinton, R., M. F. Firuzabad, and L. Bertling, 2001. Bibliography on the application of probability methods in power system reliability evaluation 1996–1999. IEEE Trans. Power Syst., 16(4): 595-602.  
 Framework for Stochastic Reliability of Bulk Power System, 1998. EPRI Rep. TR-110048. Palo Alto, CA.

- Marceau, R.J. and J. Endrenyi, 1997. CIGRE Task Force 38.03.12. Power system security assessment: A position paper", *Electra*, 175: 49-77.
- Singh, C. and J. Mitra, 1997. Composite system reliability evaluation using state space pruning. *IEEE Trans. Power Syst.*, 12(1); 471-479.
- Calley, J.M., A. Fouad, V.Vittal, A. Irizarry-Rivera, B. Agrawal and R.Farmer, 1997. A risk based security index for determining operating limits in stability-limited electric power systems. *IEEE Trans. Power Syst.*, 12(3): 1210-1219.
- Kosko, B., 1990. Fuzziness vs. Probability. *Int. J. General Systems*, 17: 211-240.
- Billinton R. and W. Li, 1992. A novel method for incorporating weather effects in composite system adequacy evaluation. *IEEE Trans. Power Syst.*, 6(3): 1154-1160.
- Bradley, E. and R.J. Tibshirani, 1994. *An Introduction to the Bootstrap*. Chapman and Hall, Inc., New York.
- Othman, M.M., A. Mohamed, and A. Hussain, 2008. Determination of Transmission Reliability Margin Using Parametric Bootstrap Technique. *IEEE Trans. on Power Syst.*, 23(4): 1689-1700.
- Alborzi, S., A. Aminian, S.M.H. Mojtahedi, and S.M. Mousavi, 2008. An analysis of project risks using the non-parametric bootstrap technique. *IEEE International Conference on Industrial Engineering and Engineering Management*, pp: 1295-1299.
- Verdonck, F., J. Jaworska, O. Thas, and P.A. Vanrollerhem, 2000. Uncertainty techniques in environmental risk assessment. *Med. Fac. Landbouww. Univ. Gent*, 65/4, pp: 247-252.
- Mili, L., Q. Qiu and A.G. Phadke, 2004. Risk Assessment of Catastrophic Failures in Electric Power System. *Int. J. Critical Infrastructures*, 1: 1.
- William, N., 2006. *Statistics for Engineers and Scientists*. New York: MacGraw Hill.
- IEEE Reliability Test System, 1979. *IEEE Transactions on Power Apparatus and Systems*, PAS-98, 6.
- Bowles, J.B. and C.E. Pelaez, 1995. Application of fuzzy logic to Reliability Engineering. In the *Proceeding of the IEEE*, 83: 3.
- Shandilya, A., H. Gupta, and J. Sharma, 1993. Method for generation rescheduling and load shedding to alleviate line overloads using local optimization. *IEE Proceedings of Generation, Transmission & Distribution*, 10: 5.
- Van Hertem, D., J. Verboomen, K.Purchala, R. Belmans, and W.L. Kling, 2005. Usefulness of DC Power Flow for Active Power Flow Analysis. *IEEE Power Engineering Society General Meeting*, 1: 454-459.
- Overbye, T.J., X. Cheng and Y. Sun, 2004. A Comparison of the AC and DC Power Flow Models for LMP Calculations. In the *Proceedings of the Hawaii International Conference on System*.
- Li, W., J. Zhou, K. Xie, and X. Xiong, 2008. Power System Risk Assessment Using a Hybrid Method of Fuzzy Set and Monte Carlo Simulation. *IEEE Transactions on Power Systems*, 23: 2.